THE JOURNAL OF BIOLOGICAL CHEMISTRY VOL. 286, NO. 3, pp. 2224–2235, January 21, 2011

Tamm-Horsfall Glycoprotein Interacts with Renal Outer Medullary Potassium Channel ROMK2 and Regulates Its Function*[S]

Received for publication, May 31, 2010, and in revised form, October 27, 2010 Published, JBC Papers in Press, November 16, 2010, DOI 10.1074/jbc.M110.149880

Aparna Renigunta[‡1], Vijay Renigunta[§], Turgay Saritas[¶], Niels Decher[§], Kerim Mutig[¶], and Siegfried Waldegger[‡2]

From the [‡]Department of Pediatric Nephrology, Children's Hospital, Philipps University of Marburg, Baldingerstr., 35043 Marburg, Germany, the [§]Institute of Physiology, Philipps University of Marburg, Deutschhausstr. 2, 35037 Marburg, Germany, and the [¶]Institute of Anatomy, Charité-University Medicine, Philippstr. 12, Berlin, Germany

Tamm-Horsfall glycoprotein (THGP) or Uromodulin is a membrane protein exclusively expressed along the thick ascending limb (TAL) and early distal convoluted tubule (DCT) of the nephron. Mutations in the THGP encoding gene result in Familial Juvenile Hyperuricemic Nephropathy (FJHN), Medullary Cystic Kidney Disease type 2 (MCKD-2), and Glomerulocystic Kidney Disease (GCKD). The physicochemical and biological properties of THGP have been studied extensively, but its physiological function in the TAL remains obscure. We performed yeast two-hybrid screening employing a human kidney cDNA library and identified THGP as a potential interaction partner of the renal outer medullary potassium channel (ROMK2), a key player in the process of salt reabsorption along the TAL. Functional analysis by electrophysiological techniques in *Xenopus* oocytes showed a strong increase in ROMK current amplitudes when co-expressed with THGP. The effect of THGP was specific for ROMK2 and did not influence current amplitudes upon co-expression with Kir2.x, inward rectifier potassium channels related to ROMK. Single channel conductance and open probability of ROMK2 were not altered by co-expression of THGP, which instead increased surface expression of ROMK2 as determined by patch clamp analysis and luminometric surface quantification, respectively. Despite preserved interaction with ROMK2, disease-causing THGP mutants failed to increase its current amplitude and surface expression. THGP$^{-/-}$ mice exhibited increased ROMK accumulation in intracellular vesicular compartments when compared with WT animals. Therefore, THGP modulation of ROMK function confers a new role of THGP on renal ion transport and may contribute to salt wasting observed in FJHN/MCKD-2/GCKD patients.

Tamm-Horsfall glycoprotein (THGP)[3] also known as Uromodulin, is the most abundant protein found in normal urine. It is localized in the luminal cell surface of the thick ascending limb (TAL) of Henle's loop and early distal convoluted tubules of the nephron (1). The mature form of the protein encompasses 616 amino acids, including 48 cysteine residues, which form the disulfide bridges responsible for its complex three-dimensional structure. THGP contains three epidermal growth factor (EGF) domains which mediate protein-protein interaction and a zona pellucida-like domain (2). It belongs to the family of GPI proteins which lack typical transmembrane domains and are anchored to the cell membrane via a c-terminal glycosylphosphatidylinositol (GPI)-anchor (3, 4).

Recent studies on physicochemical, biological, and pathological properties of THGP have unraveled its multi-faceted aspects in human health and disease. The protein via its glycans tends to form large aggregates and competes with uroplakin receptors for the adhesion of type 1 fimbriated *Escherichia coli*, and provides defense against urinary tract infections (5–7). THGP-deficient mice were shown to be severely hampered in combating colonization of bladder tissue when infected with type 1 fimbriated *E. coli* (8, 9). Moreover, THGP by reducing calcium oxalate precipitation plays a protective role with respect to renal stone formation as demonstrated by recent studies on THGP-deficient mice prone to nephrolithiasis (10, 11).

Mutations of the *THGP* gene result in three closely related kidney disorders characterized by renal salt wasting, hyperuricemia, gout and progressive renal failure (12, 13): Familial Juvenile Hyperuricemic Nephropathy (FJHN), Medullary Cystic Kidney Disease type 2 (MCKD-2), and GlomeruloCystic Kidney Disease (GCKD) (14). Detailed studies on membrane trafficking and secretion of defective THGP have clearly established that THGP mutations cause a delayed export of mutant THGP to the plasma membrane, with increased storage of THGP in the ER. To date, about 40 distinct mutations have been reported in association with these so-called THGP storage disorders (15, 16). More recently, in a genome-wide association study, the UMOD locus was identified as a major genetic susceptibility locus for chronic kidney disease (CKD), further emphasizing the importance of THGP in renal physiology (17).

* This study was supported by the Deutsche Forschungsgemeinschaft (DFG, SFB-593), Rhoen AG, and P. E. Kempkes Foundation (Grants 15/06 and 10/08, to A. R.).

[S] The on-line version of this article (available at http://www.jbc.org) contains supplemental Figs. S1–S3.

[1] To whom correspondence may be addressed. Tel.: 49-6421-58-62639/62968; Fax: 49-6421-58-65724; E-mail: renigunt@med.uni-marburg.de.

[2] To whom correspondence may be addressed. Tel.: 49-6421-58-62639/62968; Fax: 49-6421-58-65724; E-mail: siegfried.waldegger@med.uni-marburg.de.

[3] The abbreviations used are: THGP, Tamm-Horsfall glycoprotein; ROMK, renal outer medullary potassium channel; TAL, thick ascending limb; DCT, early distal convoluted tubule; FJHN, Familial Juvenile Hyperuricemic Nephropathy; MCKD-2, Medullary Cystic Kidney Disease type 2; GCKD, GlomeruloCystic Kidney Disease; m-YTH, membrane yeast two-hybrid system.

Despite various advancements in the genetics of THGP, several physiological aspects, including the possible link between THGP and ion transport in TAL as suggested by salt wasting and hyperuricemia observed in patients with THGP mutations, remain enigmatic. One of the key players in the process of NaCl reabsorption along the TAL is the potassium channel ROMK, which resides in the apical membrane of TAL cells. Via recycling of potassium ions into the tubular lumen it forms a functional unit with the apical sodium potassium chloride co-transporter (NKCC2), the rate-limiting transport protein for NaCl reabsorption along the TAL. Disturbed ROMK function thus limits TAL salt reabsorption resulting in severe renal salt wasting as observed in Bartter syndrome type II (18). Here we show that ROMK function is activated by THGP. Reduced ROMK activity thus might explain renal salt wasting in patients suffering from FJHN/MCKD-2/GCKD.

EXPERIMENTAL PROCEDURES

Molecular Cloning and Mutagenesis—Full-length hROMK2 was cloned into the pcDNA5/FRT/V5-His-TOPO TA cloning vector (Invitrogen) according to the manufacturer's protocol. Full-length hTHGP was cloned into pEGFP-C2 vector (Clontech) using HindIII and EcoR I sites. All full-length genes used for yeast two hybrid screening and direct interactions were cloned into membrane yeast two hybrid bait (pBT3C and pBT3N) and prey (pPR3C and pPR3N) vectors (MoBiTec Molecular Biotechnology, Göttingen, Germany) using SfiI sites, such that the insert is in-frame to the downstream and upstream reporter cassette respectively. All constructs (hROMK2, hTHGP, and hKir2.1), used for studies in *Xenopus* oocyte were cloned between the 5′- and 3′-UTR of the *Xenopus* β-globin gene in the modified pOG1 vector to increase expression efficiency. Chimeras were generated using overlap extension PCR method (19). For surface luminescence measurements, pOG1 vector with ROMK2 containing an external hemagglutinin (HA) epitope tag was used. QuikChange site-directed mutagenesis (Strategene, Germany) was used to introduce HA epitope tag into the extracellular loop of ROMK2 at position 112. Both ends of the epitope were flanked by PGG residues to enhance accessibility and flexibility of the extracellular HA tag, creating a sequence, which reads E111PGGYPYDVPDYAGGP.

Expression of ROMK2 in Flp-In 293 Cells—Flp-In-293 cells (Invitrogen) were co-transfected with the recombinant pcDNA5/FRT/V5-His-TOPO TA vector containing the ROMK2 gene and the pOG44 plasmid expressing the Flp recombinase gene, as described in the manufacturer's instructions (Invitrogen). Cells were incubated for 24 h to allow for expression of the hygromycin resistance gene, then selected and maintained in DMEM supplemented by fetal bovine serum (10%) and penicillin/streptomycin (1%) and hygromycin (50 μg/ml) at 37 °C under 5% CO_2. The resulting cells are described hereinafter as Flp-In-293/ROMK2 cells. ROMK2 expression in these cells was determined by electrophysiological measurements and Western blotting using anti-ROMK antibody (1:500) (Alomone Laboratories, Jerusalem, Israel).

Split-ubiquitin Membrane Yeast Two Hybrid (m-YTH) Assay—The m-YTH screening assay (MoBiTec Molecular Biotechnology, Göttingen, Germany), was performed to identify proteins that interact with ROMK2. The pBT3N-ROMK2 and ROMK2-pBT3C bait vectors were used for screening. For direct interaction studies, prey vectors containing THGP were used. Identification of positive clones, recovery of library plasmids and identification of prey sequences were performed following the manufacturer's guidelines. In brief, *Saccharomyces cerevisiae* reporter strain NMY51 was transformed with bait plasmids and the correct expression of the baits was verified by Western blot using LexA mouse monoclonal antibody (Santa Cruz Biotechnology). Verification of correct topology of the bait was performed using pAI-Alg5 and pDL2-Alg5 control preys, and the upper limit of selection stringency for screening was determined as SD *-leu/-trp/-his/-ade* (SD-LWHA) selection medium. The yeast strains expressing the baits were transformed with human kidney cDNA library (MoBiTec Molecular Biotechnology, Göttingen, Germany) for screening or with prey vectors for direct interaction studies. Protein-protein interaction was determined by growth on SD-LWHA plates. Positive colonies were further verified using the second marker β-galactosidase. The nucleotide sequence of the screened positives were determined by sequencing, and the identity of the encoded putative interacting protein was determined by database search (BLASTX).

Co-immunoprecipitation—Immunoprecipitations were carried out using Immunoprecipitation kit, Dynabeads® protein G (Invitrogen) following the manufacturer's instructions. Briefly, protein G Dynabeads were coated with rabbit anti-THP (Santa Cruz Biotechnology) under rotation for 1 h at 4 °C. Mouse kidneys were homogenized and subsequently lysed in 1× TBS Tween-20 buffer with protease inhibitor mixture (Roche) for 30 min on ice. The lysates were then centrifuged, and the supernatants were used for immunoprecipitation. Alternatively, Triton X-100 lysates prepared from HEK-293 cells or Flp-In-293/ROMK2 cells, that stably express ROMK2, transfected with either GFP tagged THGP or empty GFP constructs, were used for immunoprecipitations. In order to eliminate antibody contamination in precipitated proteins, THGP antibody was cross linked to Dynabeads protein G using the cross linking agent BS3 (Thermo Fisher Scientific) as per the manufacturer's instructions. Antibody-coated beads were incubated with the lysates under rotation for 2–3 h at 4 °C. Dynabeads coated with antigen-antibody complex were washed extensively (4×) with the wash buffer supplied by the manufacturer. The proteins on Dynabeads were eluted by boiling at 95 °C for 5 min in SDS sample loading buffer and separated on a 8% SDS-PAGE under reducing conditions. Proteins were transferred to nitrocellulose membrane and probed with either rabbit anti-THP antibody (1:1000) (Santa Cruz Biotechnology) or rabbit anti-ROMK2 antibody (1:500) (Almone). The membrane was washed and incubated with HRP-conjugated secondary antibody (1:10,000), and the bands were detected using the SuperSignal kit (Pierce).

Electrophysiological Measurements—For *Xenopus* oocyte expression studies, complementary RNA (cRNA) was transcribed *in vitro* from Not1- or SacII-linearized plasmids con-

taining the cDNA of interest using T7 RNA polymerase (mMessage mMachine T7 Kit, Ambion, Huntingdon, UK). cRNA was purified by LiCl/ethanol precipitation. Yield and concentration were quantified spectrophotometrically and the quality of RNA was confirmed by agarose gel electrophoresis. Defolliculated *Xenopus laevis* oocytes were injected with 50 nl of nuclease free water containing cRNA (10 pg/oocyte of ROMK2, Kir2.x, C1, or C2(R347A) alone or together with 10 ng/oocyte of THGP), and then stored at 16 °C in ND96 solution containing (mM) 96 NaCl, 2 KCl, 1 $MgCl_2$, 1,8 $CaCl_2$, and 5 HEPES (pH 7.4), supplemented with 100 μg/ml gentamycin and 2.5 mM sodium pyruvate. 2–3 days following injection, two-electrode voltage-clamp measurements were performed at room temperature with a Gene Clamp 500 amplifier (Axon Instruments, Union City). To establish a resting membrane potential large enough to confirm oocyte viability and establishment of adequate voltage clamp, initial electrode impalements were made in standard ND96 solution. Membrane voltage was clamped over the range −100 to +60 mV in 20 mV steps. To obtain representative inward rectification, symmetrical potassium conditions were established by replacing the bath solution with KD96 solution containing (mM) 98 KCl, 1 $MgCl_2$, 1,8 $CaCl_2$, and 5 HEPES (pH 7.4). K^+ currents were recorded in bath solution containing KD96. Statistical analysis was performed on $n = 10$ oocytes derived from one preparation. The error bars in the diagrams indicate the S.E. Experiments were repeated in at least three different batches of oocytes derived from different frogs.

Surface Luminescence Assay—Surface expression of HA-tagged ROMK2 in *Xenopus* oocytes was analyzed 2 days after injection with the cRNA (1 ng/oocyte of HA-tagged ROMK2 alone or together with 10 ng/oocyte of THGP). Oocytes were incubated for 30 min in ND96 solution containing 1% BSA at 4 °C to block nonspecific binding of antibodies. Subsequently, oocytes were incubated for 60 min at 4 °C with 1 mg/ml rat monoclonal anti-HA antibody (clone 3F10, Roche Pharmaceuticals, Basel, Switzerland) in 1% BSA/ND96, washed 6× at 4 °C with 1% BSA/ND96 and incubated with 2 mg/ml peroxidase-conjugated affinity-purified F(ab)2 fragment goat anti-rat immunoglobulinG antibody (Jackson ImmunoResearch, West Grove, PA) in 1% BSA/ND96 for 60 min. Oocytes were washed thoroughly, initially in 1% BSA/ND96 (at 4 °C for 60 min) and then in ND96 without BSA (at 4 °C for 15 min). Individual oocytes were placed in 20 μl SuperSignal Elisa Femto solution (Pierce, Chester, UK) and, after an equilibration period of 10 s, chemiluminescence was quantified in a luminometer (Lumat LB9507, Berthold Technologies, BadWildbad, Germany). For each construct surface expression of 15 oocytes was analyzed in one experiment, and at least three experiments (~40 oocytes) were carried out. The luminescence produced by water injected oocytes or oocytes expressing WT-ROMK without HA epitope was used as a reference signal (negative control). Protein immunoblotting for oocyte experiments were performed to verify equal expression of all HA-tagged ROMK2 fusion proteins in *Xenopus* oocytes. Total protein was extracted from 10 oocytes for each construct as described previously (20), and subjected to protein electrophoresis and immunoblotting. Nitrocellulose membranes were blocked overnight at room temperature in Tris-buffered saline with 0.1% Tween 20 (TBS-T) containing 5% nonfat milk (NFM). Primary (rat anti-HA monoclonal antibody (1:1000), Roche, Germany) and secondary (goat anti-rat HRP conjugate (1:5000), Jackson ImmunoResearch, West Grove, PA) antibodies were diluted in 5% NFM, incubated for 1 h each. Following each antibody incubation the membrane was washed for 10 min (3×) in TBS-T buffer. Bound antibodies were revealed using ECL plus Western blotting detection system (Amersham Biosciences, UK).

Animals, Tissues, and Treatments—Wild-type C57/Bl6 mice and $THGP^{-/-}$ mice ($n = 6$) were bred in the local animal facility and kept on standard diet and tap water. For immunohistochemical studies, adult mice were anesthetized by an intraperitoneal injection of sodium pentobarbital (0.06 mg/g body weight), their abdominal cavity was opened, and the kidneys were perfused retrogradely through the abdominal aorta using 3% paraformaldehyde (PFA) dissolved in PBS. Kidneys were then removed and 5 μm-thick cryostat sections were prepared.

KO Experiments—Methods used were as described previously (21, 22). In brief, kidney cortices were excised and homogenized in buffer-I containing 250 mM sucrose, 10 mM triethanolamine, protease inhibitors (Complete; Roche Diagnostics), and phosphatase inhibitors (phosphatase inhibitor mixture 1, Sigma) (pH 7.5). The homogenates were subjected to sequential centrifugation steps. Homogenates were centrifuged at 300 × *g* (10 min, 4 °C) to remove nuclei and whole cells. For preparation of membrane fractions, the resulting postnuclear supernatant was centrifuged at 17,000 × *g* (60 min, 4 °C) to obtain a pellet containing plasma membrane and membrane adherent vesicles (PM) and a supernatant (Ves+Cyt) containing the intracellular fraction with cytoplasmic and vesicular components. Following the removal of the large plasma membrane enriched pellet at 17,000 × *g* for 1 h, the supernatant was subsequently centrifuged at 200,000 × *g* for 1 h to obtain a vesicle-enriched pellet (Ves) and a supernatant containing cytoplasmic components (Cyt). Pellets containing the plasma membrane-enriched and vesicle-enriched fractions were dissolved in buffer-I and protein concentrations were measured using the BCA protein assay kit (Pierce). 50 μg protein/lane were run on 8% polyacrylamide minigels. After electrophoretic transfer of the proteins, polyvinylidene fluoride membranes were incubated with the primary antibody against ROMK (1:500, *Alomone*) or flotillin-1 (1:1000, BD Biosciences) (Following stripping), each for 1 h at room temperature, followed by overnight incubation at 4 °C and subsequent exposure to HRP-conjugated secondary antibodies for 2 h at room temperature. Immunoreactive bands were detected by exposure of x-ray films to chemiluminescence. The films were then scanned and evaluated densidometrically. ROMK immunoreactive signals obtained by analysis of plasma membrane-enriched fractions and vesicle-enriched fractions were normalized to flotillin-1 signals. Control blots containing PM, Ves+Cyt, Ves, and Cyt fractions were run and analyzed using primary antibodies against flotillin-1 (1:1000, BD Biosciences), β-actin (1:3000, Sigma), α-tubulin (1:2000, Sigma), and HSP-70 (1:3000, Sigma).

Immunohistochemistry—Immunohistochemical double labeling procedures were performed using goat anti-THGP (1:500) (ICN Biomedicals, Costa Mesa), rabbit anti-ROMK (1:500) (*Alomone* Laboratories, Jerusalem, Israel), and guinea pig anti-NKCC2 (1:1000) (kind gift from Dr. David Ellison, Portland, OR) primary antibodies. Cryosections were treated with 0.5% Triton X-100 in PBS for 30 min for better antigen retrieval and unspecific bindings were blocked with 5% milk powder in PBS for 30 min. The primary antibodies diluted in 5% milk powder were sequentially applied for 1 h at room temperature, followed by application of appropriate secondary fluorescent Cy3-, Cy2-conjugated antibodies (1:300) (Dianova, Hamburg, Germany) for 2 h. Sections were washed, coverslipped with PBS-glycerol, and analyzed in a Leica DMRB microscope equipped with a SPOT 32 camera and MetaView 3.6a software (Diagnostic Instruments; Universal Imaging) or a Zeiss confocal microscope (LSM 5 Exciter).

Statistical Tests—Data are reported as means ±S.E. Statistical significance was determined using Student's *t* test. In the figures, statistically significant differences to control values are marked by *asterisks* (*, $p < 0.01$; **, $p < 0.001$; and ***, $p < 0.0001$); *n.s* indicates non-significant differences ($p > 0.05$).

RESULTS

Identification and Verification of THGP as ROMK2-interacting Protein—We performed a membrane yeast two-hybrid screen against a human kidney cDNA library, using ROMK2 as the bait with the C-terminal ubiquitin (Cub) fused to the N terminus of ROMK2 in one set and to the C terminus of ROMK2 in another set of screening (Fig. 1*A*, *left*). Screening over 1000 clones revealed THGP as a potential ROMK2-interacting protein. As expected, full-length THGP fused to the N-terminal ubiquitin (Nub) gave a positive interaction signal in the split-ubiquitin yeast two-hybrid assay upon expression with both the ROMK baits, yielding a $his^+/ade^+/lacZ^+$ phenotype in the yeast NMY51 strain (Fig. 1*A*, *right*). To further verify ROMK2-THGP interaction, we performed co-localization and co-immunoprecipitation experiments. As expected, immunostaining of mouse kidney sections revealed strong ROMK signal in the TAL and DCT and weak signal in CCD in both WT and $THGP^{-/-}$ animals (Fig. 6*D*). We observed a strong THGP signal in the TAL of wild-type mouse and absence of THGP signal in the $THGP^{-/-}$ mouse. Co-staining of mouse kidney sections resulted in partial co-localization of both ROMK and THGP signals in the luminal and ad-luminal membranes of wild-type mouse TAL-cells (Fig. 1*B*). Co-immunoprecipitation experiments were performed using total protein lysate extracted from mouse kidneys of both wild-type and $THGP^{-/-}$ animals. Indeed, we identified ROMK protein in the anti-THGP immunoprecipitate of wild-type animals, whereas no ROMK protein was detected in that of $THGP^{-/-}$ animals (Fig. 1*C*). In a separate batch of experiments we demonstrated that ROMK and THGP co-immunoprecipitated when heterologously expressed in mammalian cells. Co-immunoprecipitation experiments were performed using cell lysates from HEK-293 cell line stably expressing ROMK and transfected with either GFP tagged THGP or empty GFP (negative control). Furthermore, HEK-293 cell lysate was used to demonstrate anti-ROMK antibody specificity. We detected ROMK protein in the anti-THGP immunoprecipitate of HEK-293 cells expressing ROMK and GFP-tagged THGP whereas no ROMK protein was detected in the anti-THGP immunoprecipitate of HEK-293 cells expressing ROMK and empty GFP (Fig. 1*D*).

Functional Consequences of the Interaction between THGP and ROMK2—To investigate the functional relevance of ROMK2 and THGP interaction we performed electrophysiological measurements in *Xenopus* oocytes with two-electrode voltage-clamp (TEVC) analysis. In contrast to THGP, expression of ROMK2 induced measurable potassium currents with expected weak inward rectification. As shown in Fig. 2, *A–C*, expression of ROMK2 together with THGP significantly increased ROMK current amplitude in the order of ~4-fold.

Single channel recordings (see supplemental Fig. S1) suggested an increased surface expression of ROMK2 in the presence of THGP. We therefore investigated the effect of THGP on ROMK2 surface expression. To this end we employed hemagglutinin (HA)-tagged ROMK2 to quantify ROMK surface expression in the absence and presence of THGP in *Xenopus* oocytes. When expressed in *Xenopus* oocytes, HA-tagged ROMK2 yielded currents identical to those observed for the wild-type channel with comparable activation when expressed with THGP (data not shown). Expression of the extracellularly tagged ROMK2 construct in *Xenopus* oocytes revealed a robust luminescence signal when compared with oocytes expressing wild type ROMK2 without HA-epitope (data not shown). Upon co-expression with THGP we observed a nearly 3-fold increase in the surface expression of ROMK2 (Fig. 2, *D* and *E*). This increase in surface expression of ROMK2 protein therefore provided an explanation for the increased ROMK current amplitude in the presence of THGP.

Effect of THGP Is Specific to ROMK and Is Mediated by the ROMK C Terminus—To check whether the effect of THGP is specific for ROMK2 (Kir1.1b), we co-expressed THGP with Kir2.1, Kir2.3, and Kir2.4, other members of the Kir family of inwardly rectifying potassium channels. As previously reported (23, 24), Kir2.x channels expressed in *Xenopus* oocytes gave rise to potassium currents with more pronounced inward rectification as compared with ROMK2. In contrast to ROMK2, expression of Kir2.x together with THGP did not change their current amplitudes (Fig. 3). Taken together, our data suggest that THGP specifically influences ROMK channels, leading to enhanced current amplitudes. This effect seemed to depend on the C terminus of ROMK. Swapping the C terminus of Kir2.1 with that of ROMK resulted in the transplantation of the THGP effect on Kir2.1, which in its native form was not activated by THGP (see supplemental Fig. S2).

Interaction of THGP Mutants with ROMK2—Among the 40 different THGP mutations reported so far, we analyzed five representative mutations localized in the epidermal growth factor (EGF)-like domain (D59A and N128S), in the central portion including the D8C domain (C150S and C217R) and in the *zona pellucida* (ZP) domain (C347G) (Fig. 4*A*). These mu-

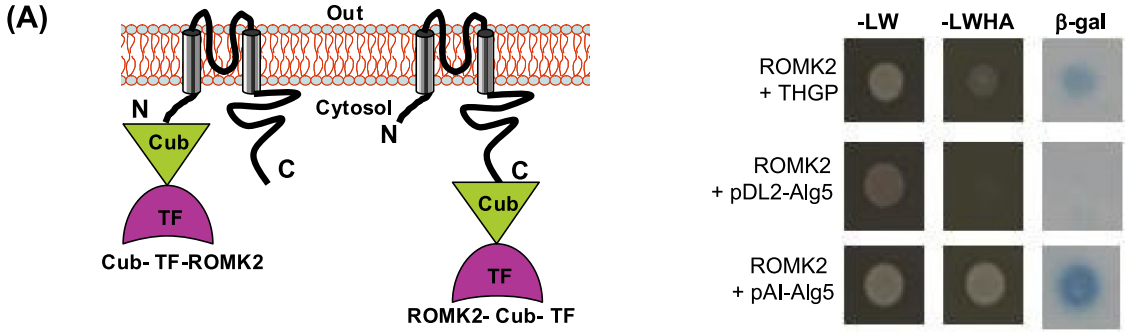
(A)
Out
Cytosol
N
Cub
C
TF
Cub- TF-ROMK2
ROMK2- Cub- TF
-LW
-LWHA
β-gal
ROMK2
+ THGP
ROMK2
+ pDL2-Alg5
ROMK2
+ pAI-Alg5

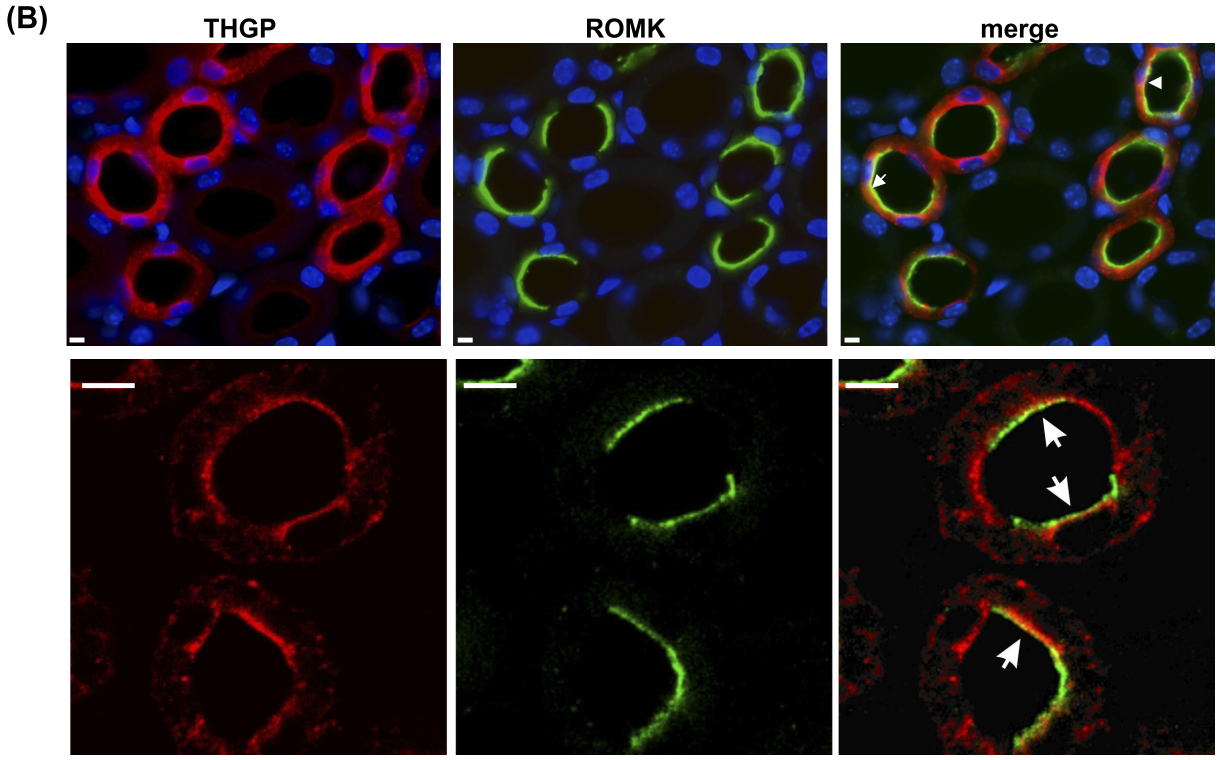
(B)
THGP
ROMK
merge

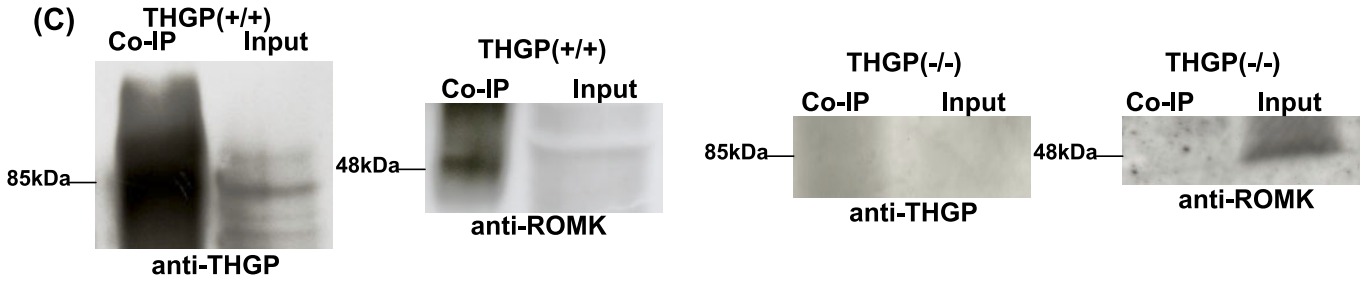
(C)
THGP(+/+)
Co-IP
Input
85kDa
anti-THGP
THGP(+/+)
Co-IP
Input
48kDa
anti-ROMK
THGP(-/-)
Co-IP
Input
85kDa
anti-THGP
THGP(-/-)
Co-IP
Input
48kDa
anti-ROMK

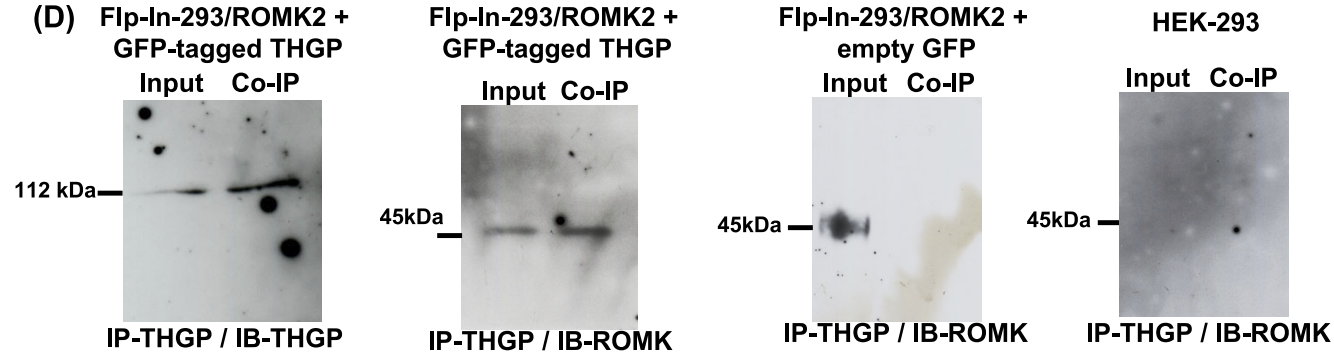
(D)
Flp-In-293/ROMK2 +
GFP-tagged THGP
Input Co-IP
112 kDa
IP-THGP / IB-THGP
Flp-In-293/ROMK2 +
GFP-tagged THGP
Input Co-IP
45kDa
IP-THGP / IB-ROMK
Flp-In-293/ROMK2 +
empty GFP
Input Co-IP
45kDa
IP-THGP / IB-ROMK
HEK-293
Input Co-IP
45kDa
IP-THGP / IB-ROMK

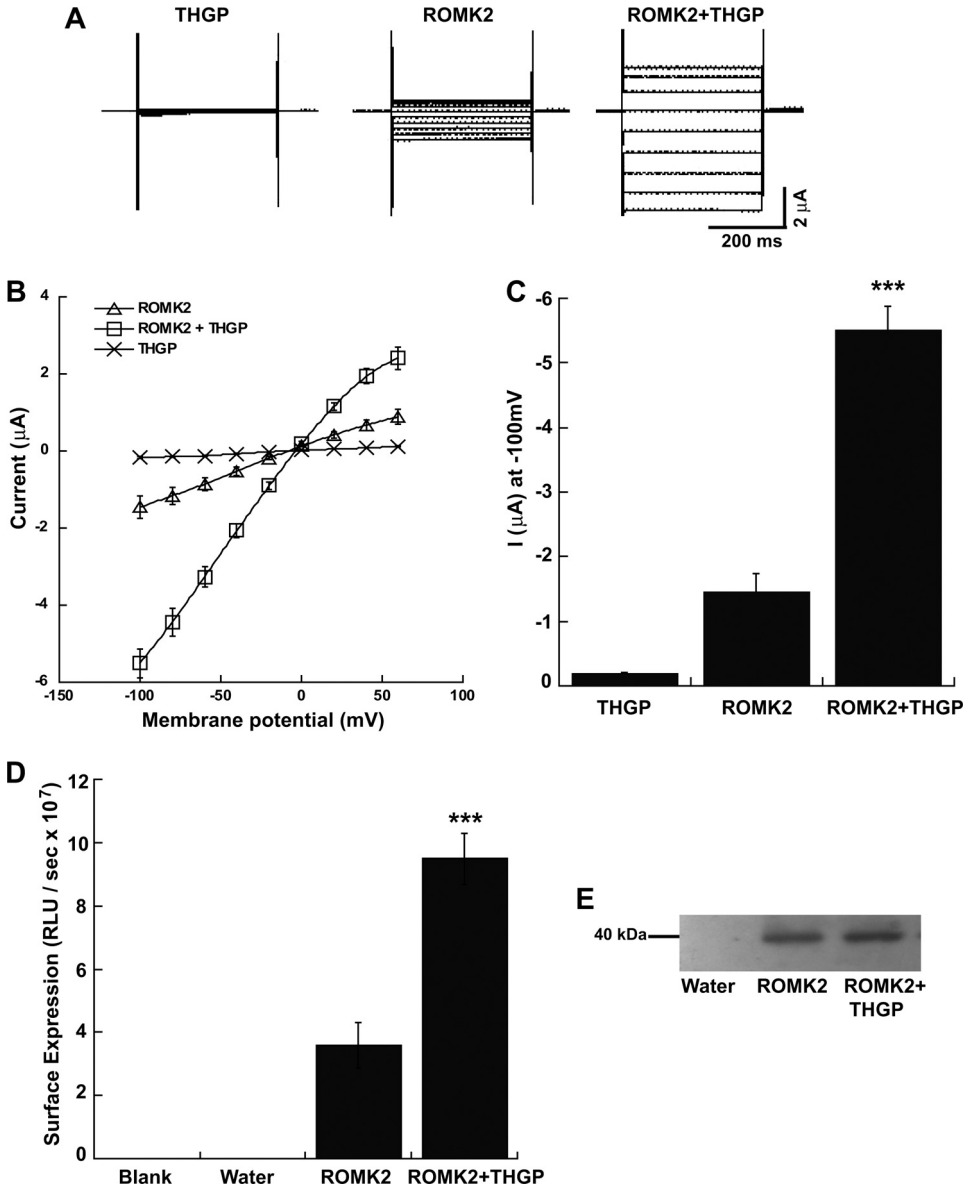

FIGURE 2. **Effect of THGP on ROMK currents.** *A*, representative whole cell currents from *Xenopus* oocytes injected with ROMK2 (*left*) or THGP (middle) or both (*right*) are shown. *B*, macroscopic current-voltage relationships and *C*, currents activated at −100mV were plotted. *D*, *Xenopus* oocytes injected with HA-tagged ROMK2 alone or together with THGP were assayed for surface expression, as determined by a cell surface luminescence assay. *E*, corresponding Western blots of HA-tagged protein in total oocyte lysates. Water-injected oocytes were taken as control to determine antibody specificity ($n = 15$, ***, $p <$ 0.0001 *versus* ROMK2).

tations were previously reported to lead to defective trafficking of mutant THGP to the plasma membrane due to ER retention (15). Co-expressing ROMK2 bait with THGP (WT and mutant isoforms) preys yielded $his^+/ade^+/lacZ^+$ phenotypes in the yeast NMY51 strain (Fig. 4*B*). Therefore, disease-causing mutations of THGP did not interfere with its interaction with ROMK2. Moreover, all examined mutant forms of THGP interacted with ROMK2 with comparable strengths as that of WT-THGP (as depicted by relative β-gal activity measurements, data not shown).

FIGURE 1. **ROMK2 interacts with THGP.** *A*, membrane yeast two hybrid (m-*YTH*) constructs used in this study. ROMK2 fused to the C-terminal half of ubiquitin (*Cub*) along with an artificial transcriptional factor (*TF*) is in-frame to the upstream and downstream reporter cassette respectively were used as baits (*left*). Y2H assays showing interaction between ROMK2 and THGP. Shown are plates with selective medium (SD) lacking leucine and tryptophan (−LW), indicating the transforming of both bait and prey vectors; with SD−LWHA, indicating the expression of reporter genes *HIS3* and *ADE2*; and with β-galactosidase as a second reporter assay, indicating positive interaction. ROMK2 was also co-transformed with negative (pDL2-Alg5) and positive (pAl-Alg5) control preys (*right*). *B*, fluorescence (*upper panel*) and confocal (*lower panel*) images show immunohistochemical co-localization of THGP and ROMK in the medullary thick ascending limb (*TAL*) of mouse kidney revealing double immunostaining for THGP (*red*) and ROMK (*green*). Merging THGP and ROMK staining revealed partial overlap of the signals within the mouse TAL cells, indicated by *arrows*. All images are supplemented with scale bars (10 μm). *C*, total kidney lysates of wild-type and $THGP^{-/-}$ mice were prepared and subjected to immunoprecipitation using anti-THGP antibody and the blots were probed with anti-ROMK antibody. *D*, Flp-In-293/ROMK2 stable cells were transfected with GFP-tagged THGP or empty GFP constructs. Cell lysates were immunoprecipitated with anti-THGP antibody, and immunoblotted with anti-ROMK antibody. HEK-293 cell lysate was used to verify the specificity of anti-ROMK antibody.

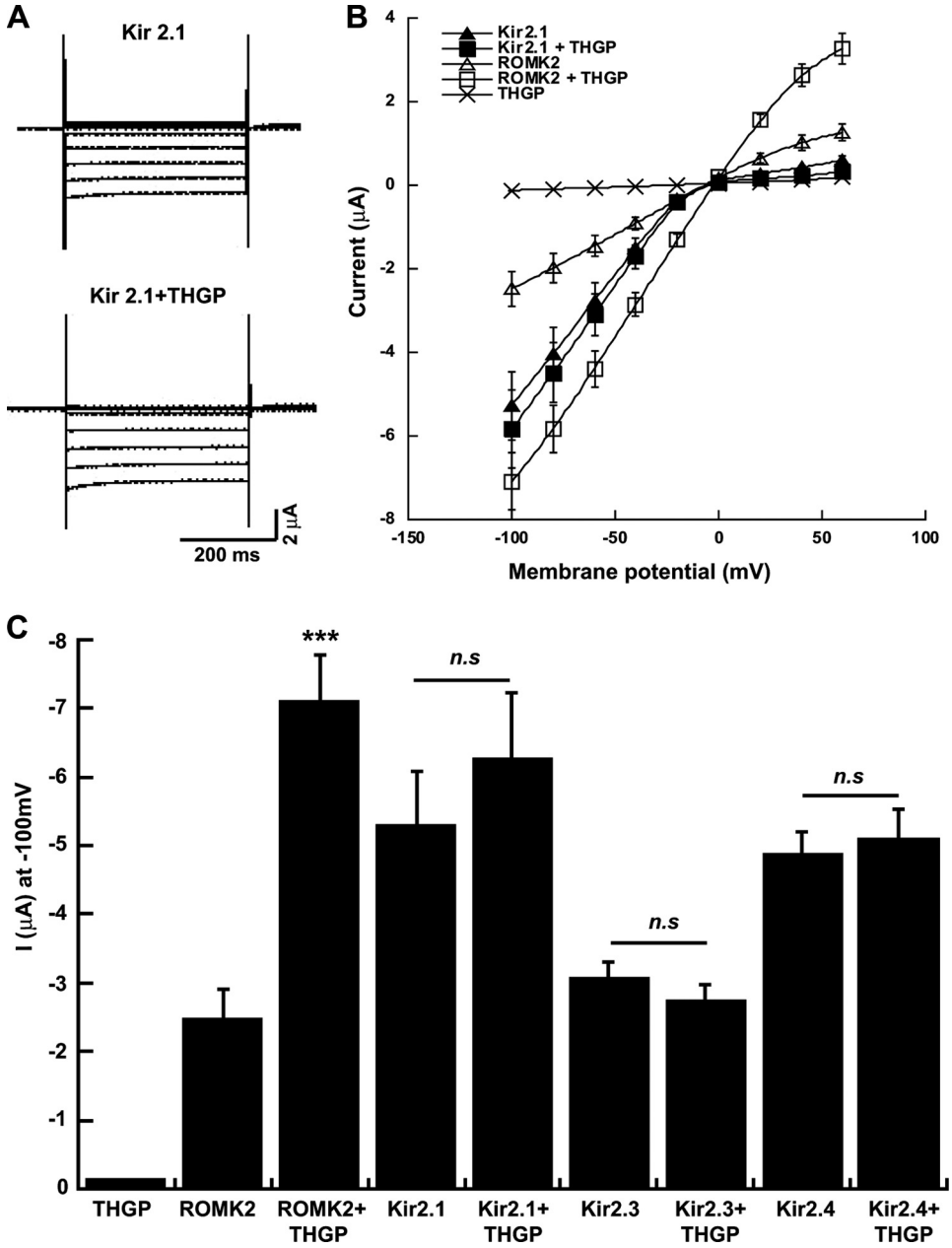

FIGURE 3. **Effect of THGP on Kir2. x inward rectifier potassium channels.** *A*, representative whole cell currents from *Xenopus* oocytes co-injected with Kir2.1 and THGP are shown. *B*, corresponding macroscopic current-voltage relationships and *C*, currents activated at −100mV were plotted for three different Kir2.x (2.1, 2.3, and 2.4) potassium channels. $n = 10$, ***, $p < 0.0001$ *versus* ROMK2, *n.s*: not significant.

Effect of Disease-causing THGP Mutations on ROMK2—Next we analyzed if THGP mutants effect ROMK2 currents and its surface expression. Co-expression of cRNAs encoding ROMK2 and WT-THGP significantly increased ROMK current amplitudes. In-contrast, none of the tested disease-causing THGP mutants activated ROMK currents (Fig. 5, *A* and *B*). Consistent with these functional data, surface quantification of HA-ROMK2 expression after co-expression with THGP mutants revealed a significant decrease in ROMK2 surface expression as compared with WT-THGP (Fig. 5*C*). Thus, disease-causing THGP mutants fail to activate current amplitudes and surface expression of ROMK2.

ROMK Expression in THGP$^{-/-}$ Mouse—Previous studies on knock-out mice lacking THGP revealed reduced ability to concentrate urine under water deprivation and altered renal salt handling (10, 25, 26). It has been proposed that these changes may be a direct consequence of a defect in NaCl reabsorption due to THGP depletion in the TAL (10). With ROMK as one of the essential TAL transporters involved in NaCl reabsorption, our data could suggest that the defect in NaCl reabsorption in these KO animals is a result of disturbed ROMK channel function. To answer this, we evaluated ROMK expression in THGP knock out mice. We performed semiquantitative protein immunoblot evaluation of ROMK in six representative THGP$^{-/-}$ mice and their wild-type littermates (Fig. 6*A*). Representative Western blots from kidney homogenates of WT mice showing the distribution of compartment-specific control proteins demonstrate the purity of

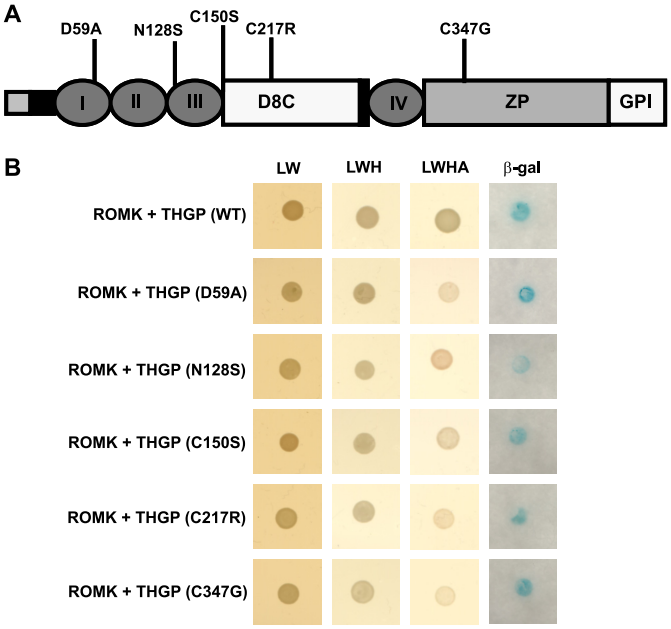

FIGURE 4. **THGP mutants interact with ROMK2.** *A*, schematic representation of THGP domain organization. *I-IV* are the epidermal growth factor-like domains; *D8C*, domain containing the eight conserved cysteine residues; *ZP*, zona pellucida domain responsible for the polymerization of extracellular proteins; *GPI*, site of GPI anchor attachment. The positions of the five THGP mutations that were analyzed in this study are shown. *B*, Y2H assays showing interaction between ROMK2 and THGP WT and mutants. Shown are plates with selective medium lacking leucine and tryptophan (−LW), indicating the transforming of both bait and prey vectors; with SD−LWH and SD−LWHA, indicating the expression of reporter genes *HIS3* and *ADE2*; and with β-galactosidase as a second reporter assay. Growth of yeast cells in SD−LWH, SD−LWHA and β-gal plates indicate positive interaction.

the plasma membrane-enriched and vesicle-enriched preparations (Fig. 6*B*). Densidometric analysis of ROMK Western blots obtained from the plasma membrane- and vesicle-enriched preparations from total kidney homogenates revealed a decrease in ROMK immunoreactivity in the plasma membrane-enriched fractions (−24%, $p < 0.01$) and a significant increase in ROMK immunoreactivity in the vesicle-enriched fractions (+86.17%, $p < 0.001$) obtained from THGP$^{-/-}$ kidneys over that of wild-type animals (Fig. 6*C*). In line with these Western blot data, analysis of ROMK protein distribution by regular immunofluorescence, as well as by confocal imaging on kidney slices revealed a more diffuse staining pattern of ROMK in the TAL tubules of the THGP$^{-/-}$ mice when compared with the sharp membrane staining of ROMK in the wild-type mice. ROMK staining in the cortical collecting duct (CCD), which is devoid of THGP expression was used as a negative control. As expected, we did not observe any difference in membrane staining of CCD cells between the WT and THGP$^{-/-}$ mice (Fig. 6*D*). Therefore, our data indicate that there is a decrease in the plasma membrane fraction of ROMK in THGP$^{-/-}$ mice because of a pronounced accumulation of ROMK in the vesicular compartment of the TAL in these animals.

DISCUSSION

In a quest to identify novel genes associated with renal salt handling, we screened a kidney library for proteins interacting with ROMK2, a potassium channel with a major role in renal tubular salt re-absorption. We identified THGP as a ROMK2-interacting protein, regulating its function by increasing its membrane expression. This effect was not observed with THGP mutations associated with diverse inherited forms of cystic kidney diseases accompanied by renal salt wasting.

THGP was first described more than 50 years ago (27). Much is known about the physico-chemical and biological properties of THGP, but its physiological role still remains not fully understood. Here, we identified THGP as an interacting partner of ROMK2, using a membrane yeast two hybrid (m-YTH) system. The protein-protein interaction was further verified by co-localization and co-immunoprecipitation studies. Co-injecting *Xenopus* oocytes with ROMK2 and THGP, strongly increased ROMK current amplitudes. Furthermore, yeast two hybrid results showed that THGP did not interact with Kir2.1, another closely related inward rectifier potassium channel. In *Xenopus* oocytes, co-expressing THGP with three other inward rectifier potassium channels belonging to Kir2.x family (2.1, 2.3, and 2.4) did not influence their currents, thus pointing toward a specific effect of THGP on ROMK2. Absence of both, interaction and influence on channel activity of THGP on Kir2.x, clearly indicates that the sticky nature of THGP by which it tends to form gel-like mucoid polymers when secreted in urine, is not the cause for protein-protein interaction between THGP and ROMK2. At this point, although there is compelling evidence for ROMK2-THGP interaction both from *in vitro* and *in vivo* studies, the detailed mechanism of how this interaction takes place in view of the topology of the two proteins remains unclear. Previous studies have shown that the machinery required for the ER exit of GPI-anchored proteins have additional functions in trafficking of transmembrane proteins. Deletion of Erv14p, a protein that affects maturation and trafficking of GPI-anchored proteins (28, 29), leads to ER retention of transmembrane proteins Ax12p (30) and Sma1p (31). Also, recent studies have described an association between Kir channels (Kir3.2) and proteins that affect maturation and trafficking of GPI-anchored proteins. They have demonstrated that Kir channel trafficking is influenced by indirect effects on GPI-anchored proteins. The study also speculated that the interplay between different classes of proteins during the formation of lipid microdomains may affect trafficking of Kir channels (29). Additionally, recent findings in *Drosophila* stated that, a GPI anchor protein (sleep-promoting factor, SSS) regulates the activity of a potassium channel of the shaker family, thus arguing in favor of modulation of membrane-bound ion channel activity by GPI-anchored extracellularly bound plasma membrane proteins (32). There is now growing evidence to demonstrate that certain secretory proteins and membrane spanning ion channels are associated with discrete domains enriched in glycophospholipids and cholesterol, called lipid rafts. Previous studies have demonstrated the presence of human THGP in lipid rafts (33, 34). THGP was shown to co-localize with NKCC2 in the lipid rafts of the TAL cell membranes (34). Other studies have demonstrated that also Kir channels are associated with lipid rafts (35) and that a conserved C-terminal region contains a unique lipid interaction domain (36). Our m-YTH and *Xenopus* ex-

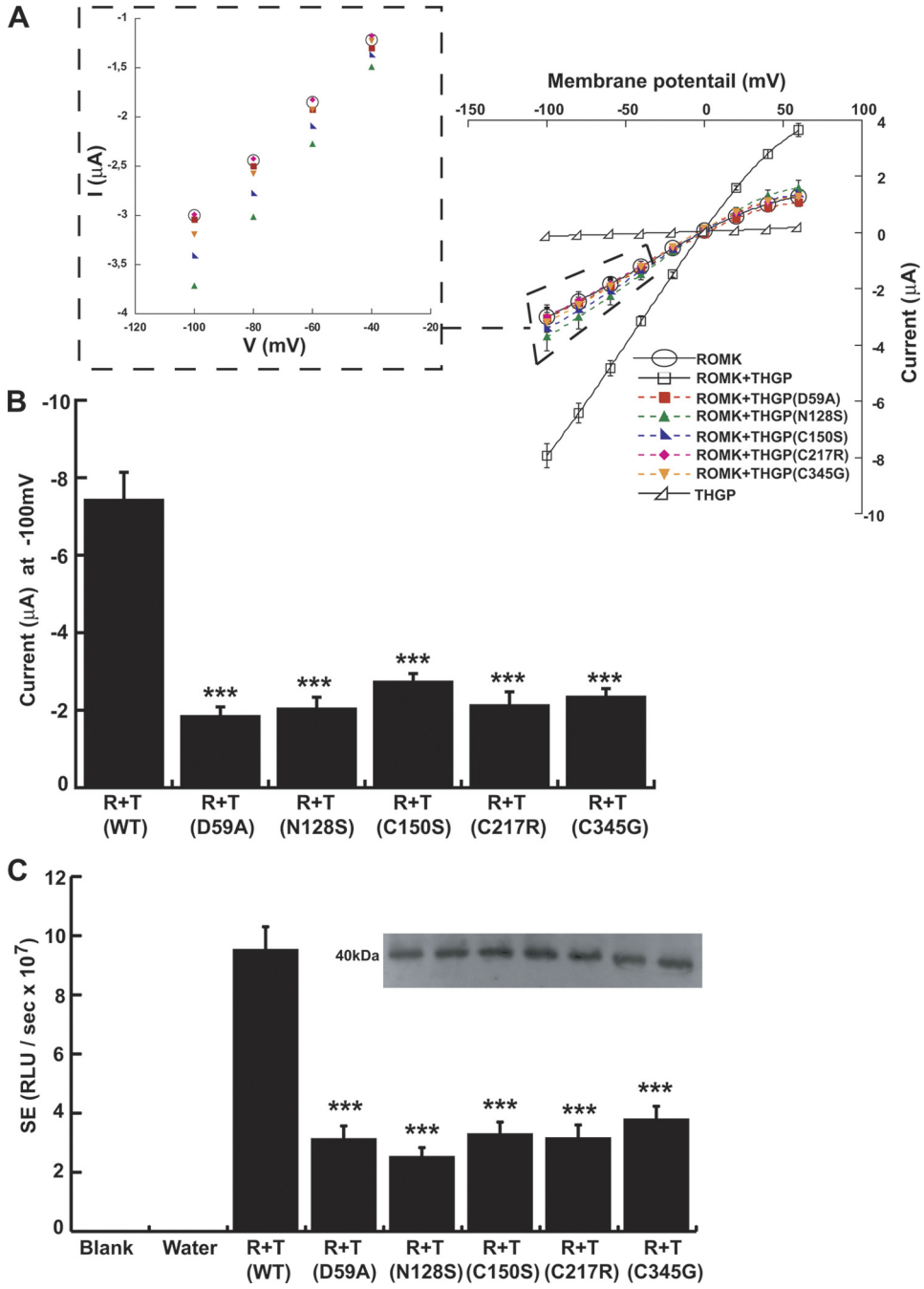

FIGURE 5. **Effect of THGP mutants on ROMK2.** *A*, macroscopic whole cell current-voltage relationships and *B*, currents activated at −100 mV were plotted for *Xenopus* oocytes co-injected with ROMK2 (*R*) and THGP (*T*) mutants. *C*, *Xenopus* oocytes co-injected with HA-tagged ROMK2 and THGP (WT or mutants) were assayed for surface expression, as measured by a cell surface luminescence assay. The *inset* contains the corresponding Western blots of HA-tagged protein in the total oocyte lysates. $n = 15$, ***, $p < 0.0001$ *versus* ROMK2+THGP.

pression studies employing ROMK2/Kir2.1 chimeras, C1 and C2(R347A) containing ROMK2 with its C terminus replaced with that of Kir2.1 and Kir2.1 with its C terminus replaced with that of ROMK2, respectively, revealed that, particularly the C terminus of ROMK2 is essential for interaction with and regulation of channel function by THGP. Therefore, it is tempting to hypothesize that the interaction between THGP and ROMK2 is mediated via lipid rafts and the C terminus of ROMK2 is essential for its assembly into these membrane microdomains.

Electrophysiological studies and knock-out mouse models have shown that TAL cells exhibit apical small conductance (30 pS) and intermediate conductance (70 pS) Kir channels, both of which are related to ROMK. Studies have also suggested that the 70 pS K-channel is a heterotetramer including ROMK and an unidentified subunit (37, 38). Our functional data along with the specific nephronal location of both ROMK2 and THGP in the apical membrane of TAL-cells (1), prompted us to speculate that THGP might constitute the missing subunit of the ROMK potassium channel. However,

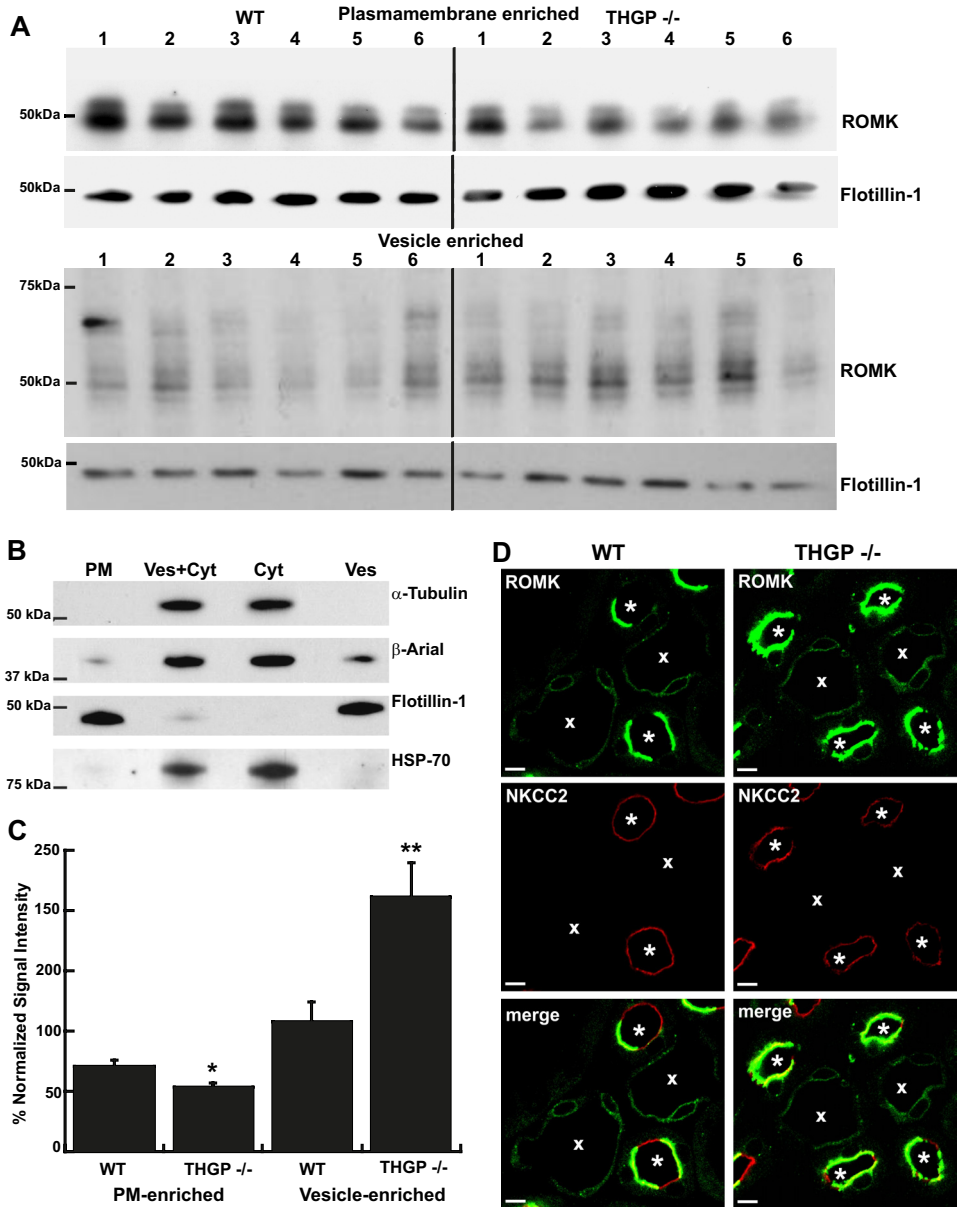

FIGURE 6. **ROMK expression in THGP$^{-/-}$ mice.** *A*, Western blots from the TAL cell extracts of WT and THGP$^{-/-}$ mice ($n = 6$ animals each) show specific bands for ROMK in the plasma membrane- and vesicle-enriched fractions. Corresponding control flotillin-1 blots for plasma membrane- and vesicle-enriched fractions are represented. *B*, representative Western blots from kidney homogenates of WT mouse ($n = 6$ animals) show specific bands for α-tubulin, β-actin, flotillin-1, and HSP-70 in the plasma membrane (*PM*; 17,000 $\times$ *g*, pellet), vesicle and cytosol- (*Ves*+*Cyt*; 17,000 $\times$ *g*, supernatant) cytosol (*Cyt*; 200,000 $\times$ *g*, supernatant) and vesicle-enriched fractions (200,000 $\times$ *g*, pellet). Note the nearly complete to absolute absence of signal for cytoskeleton (α-tubulin, β-actin) and cytosolic (HSP-70) proteins in membrane-enriched fractions, whereas membrane resident protein Flotillin-1 was mainly distributed in membrane-enriched fractions clearly demonstrating the purity of plasma membrane and vesicle preparations. *C*, densitometric analysis of Western blots with intensity values normalized to flotillin for plasma membrane- and vesicle-enriched fractions are plotted for both strains ($n = 6$, *, $p < 0.01$; **, $p < 0.001$ *versus* WT). *D*, confocal images show a sharp membrane staining of ROMK in the wild-type mice, whereas THGP$^{-/-}$ mice show a diffuse staining pattern of ROMK in the TAL tubules. TAL cells (*) were identified by co-staining for NKCC2, a sodium-potassium-chloride transporter specifically expressed along the TAL. ROMK staining in CCD cells (×) lacking expression of THGP and NKCC2 serves as a negative control. Phase contrast images of TAL and CCD for both WT and THGP$^{-/-}$ mice are provided in supplemental Fig. S3). All images are supplemented with scale bars (10 μm).

as shown by our single channel recordings, ROMK single channel conductance was not altered by THGP, ruling out its role as an integral part of the ROMK potassium channel. Yet, whole cell and single channel recordings indicated that the increase in channel activity may arise from an increase in the surface expression of ROMK2 in the presence of THGP. This indeed was confirmed by our surface luminescence assay in *Xenopus* oocytes using a HA-tagged ROMK2 construct. Interestingly, THGP has two protein domains that aid in apical sorting, namely an N-terminal leader peptide (14) and a C-terminal GPI-anchor (39). Therefore, association of THGP with ROMK in TAL cells may thus aid in apical sorting of ROMK, which by itself lacks an apical sorting signal.

In recent years attention has been drawn toward human diseases associated with THGP mutations including familial juvenile hyperuricemic nephropathy (FJHN), medullary cystic kidney disease type 2 (MCKD-2) and glomerulocystic kidney disease (GCKD), presenting with renal salt wasting, hyperuri-

caemia, gout, and end stage renal failure (12–14, 40). In affected patients, a mutant form of THGP is produced which is retained in the ER (THGP storage disease) and decreases the amount and rate of THGP secretion in the urine. To date more than 40 THGP mutations have been identified (15, 16). Despite these advancements in the genetics of THGP storage diseases, several physiological aspects of these diseases, especially the putative link between THGP protein, renal salt wasting, and uric acid handling remain enigmatic. On these lines, as a further step in understanding THGP biology in human health and disease, we analyzed 5 representative disease causing mutations localized in different domains of the protein. All mutations were previously reported to result in delayed trafficking of mutant THGP to the plasma membrane due to ER retention (15). Other studies in yeast cells demonstrated that, delayed ER exit of GPI-anchored proteins disrupt the formation of lipid domains in ER and thereby indirectly affect sorting and transport of transmembrane proteins (41). In accordance with these findings in yeast cells demonstrating the indirect effect of GPI-anchored proteins on ion channel trafficking (29, 41), we observed that although all examined mutant forms of THGP interacted with ROMK2 with comparable strengths as that of WT-THGP, studies in *Xenopus* oocyte showed that mutant isoforms of THGP when co-expressed with ROMK2 failed to increase ROMK current amplitudes and its surface expression. Therefore, we hypothesize that renal salt wasting observed in patients with THGP storage diseases may result from an indirect effect of ER accumulation of THGP on ROMK surface expression.

The role of THGP in renal salt handling has been studied employing knockout animals. THGP$^{-/-}$ mice showed normal glomeruli and tubular segments with no evidence of interstitial fibrosis or cell injury unlike patients suffering from THGP storage diseases. Two independent studies on THGP$^{-/-}$ mice reported moderate disturbances of renal electrolyte handling in KO animals compared with their wild-type litter mates (10, 26). Also, because severe renal salt wasting is a hallmark of ROMK dysfunction as observed in patients suffering from Bartter syndrome (18), we checked for ROMK expression in THGP$^{-/-}$ mice. Because THGP is completely absent in these animals we speculated a decrease or delay in ROMK transport to the apical cell membrane. Indeed, we observed a decrease in the ROMK immunoreactivity in the plasma membrane-enriched fractions and marked increase in ROMK immunoreactivity in the vesicle-enriched fractions of the THGP$^{-/-}$ kidneys over their wild-type littermates. A previous study on characterization of renal changes associated with genetic ablation of THGP in mice, demonstrated an increase in the renal expression of ROMK (26). Therefore, These observations together with our KO studies tempts us to speculate that THGP ablation results in a large accumulation of ROMK in the vesicles thereby resulting in a delay or decrease in the surface expression of ROMK. This decrease in ROMK surface expression therefore explains the milder phenotype for salt wasting in THGP deficiency as opposed to severe salt wasting observed in total dysfunction or deficiency of ROMK as in Bartter syndrome. Taken together, our data provide the first evidence that THGP participates in renal sodium transport via ROMK channel regulation. This adds a new dimension to the multifaceted roles of THGP in human health and disease.

Acknowledgments—We thank Anne Kathrin Streit for oocyte single channel measurements. We are grateful to Dr. Satish Kumar for providing the THGP$^{-/-}$ mouse. We would like to thank Prof. Dr. Sebastian Bachmann and Prof. Jürgen Daut for useful discussions. We would like to thank Christina Rösser, Kirsten Ramlow, and Doris Wagner for excellent technical support.

REFERENCES

1. Malagolini, N., Cavallone, D., and Serafini-Cessi, F. (1997) *Kidney Int.* **52,** 1340–1350
2. Devuyst, O., Dahan, K., and Pirson, Y. (2005) *Nephrol. Dial Transplant.* **20,** 1290–1294
3. Rindler, M. J., Naik, S. S., Li, N., Hoops, T. C., and Peraldi, M. N. (1990) *J. Biol. Chem.* **265,** 20784–20789
4. Cavallone, D., Malagolini, N., and Serafini-Cessi, F. (2001) *Biochem. Biophys. Res. Commun.* **280,** 110–114
5. Orskov, I., Ferencz, A., and Orskov, F. (1980) *Lancet* **1,** 887
6. Dulawa, J., Jann, K., Thomsen, M., Rambausek, M., and Ritz, E. (1988) *Eur J. Clin. Invest.* **18,** 87–91
7. Pak, J., Pu, Y., Zhang, Z. T., Hasty, D. L., and Wu, X. R. (2001) *J. Biol. Chem.* **276,** 9924–9930
8. Mo, L., Zhu, X. H., Huang, H. Y., Shapiro, E., Hasty, D. L., and Wu, X. R. (2004) *Am. J. Physiol. Renal Physiol.* **286,** F795–F802
9. Bates, J. M., Raffi, H. M., Prasadan, K., Mascarenhas, R., Laszik, Z., Maeda, N., Hultgren, S. J., and Kumar, S. (2004) *Kidney Int.* **65,** 791–797
10. Mo, L., Liaw, L., Evan, A. P., Sommer, A. J., Lieske, J. C., and Wu, X. R. (2007) *Am. J. Physiol. Renal Physiol.* **293,** F1935–F1943
11. Carvalho, M., Mulinari, R. A., and Nakagawa, Y. (2002) *Braz. J. Med. Biol. Res.* **35,** 1165–1172
12. Hart, T. C., Gorry, M. C., Hart, P. S., Woodard, A. S., Shihabi, Z., Sandhu, J., Shirts, B., Xu, L., Zhu, H., Barmada, M. M., and Bleyer, A. J. (2002) *J. Med. Genet.* **39,** 882–892
13. Scolari, F., Caridi, G., Rampoldi, L., Tardanico, R., Izzi, C., Pirulli, D., Amoroso, A., Casari, G., and Ghiggeri, G. M. (2004) *Am. J. Kidney Dis.* **44,** 987–999
14. Rampoldi, L., Caridi, G., Santon, D., Boaretto, F., Bernascone, I., Lamorte, G., Tardanico, R., Dagnino, M., Colussi, G., Scolari, F., Ghiggeri, G. M., Amoroso, A., and Casari, G. (2003) *Hum. Mol. Genet.* **12,** 3369–3384
15. Bernascone, I., Vavassori, S., Di Pentima, A., Santambrogio, S., Lamorte, G., Amoroso, A., Scolari, F., Ghiggeri, G. M., Casari, G., Polishchuk, R., and Rampoldi, L. (2006) *Traffic* **7,** 1567–1579
16. Jennings, P., Aydin, S., Kotanko, P., Lechner, J., Lhotta, K., Williams, S., Thakker, R. V., and Pfaller, W. (2007) *J. Am. Soc. Nephrol.* **18,** 264–273
17. Köttgen, A., Glazer, N. L., Dehghan, A., Hwang, S. J., Katz, R., Li, M., Yang, Q., Gudnason, V., Launer, L. J., Harris, T. B., Smith, A. V., Arking, D. E., Astor, B. C., Boerwinkle, E., Ehret, G. B., Ruczinski, I., Scharpf, R. B., Ida Chen, Y. D., de Boer, I. H., Haritunians, T., Lumley, T., Sarnak, M., Siscovick, D., Benjamin, E. J., Levy, D., Upadhyay, A., Aulchenko, Y. S., Hofman, A., Rivadeneira, F., Uitterlinden, A. G., van Duijn, C. M., Chasman, D. I., Pare, G., Ridker, P. M., Kao, W. H., Witteman, J. C., Coresh, J., Shlipak, M. G., and Fox, C. S. (2009) *Nat. Genet.* **41,** 712–717
18. Simon, D. B., Karet, F. E., Rodriguez-Soriano, J., Hamdan, J. H., DiPietro, A., Trachtman, H., Sanjad, S. A., and Lifton, R. P. (1996) *Nat. Genet.* **14,** 152–156
19. Ho, S. N., Hunt, H. D., Horton, R. M., Pullen, J. K., and Pease, L. R. (1989) *Gene* **77,** 51–59
20. Zuzarte, M., Rinné, S., Schlichthörl, G., Schubert, A., Daut, J., and Preisig-Müller, R. (2007) *Traffic* **8,** 1093–1100
21. Schmitt, R., Kahl, T., Mutig, K., and Bachmann, S. (2004) *Histochem. Cell Biol.* **121,** 319–327
22. Sachs, A. N., Pisitkun, T., Hoffert, J. D., Yu, M. J., and Knepper, M. A.

(2008) *Am. J. Physiol. Renal Physiol.* **295,** F1799–F1806
23. Kubo, Y., Baldwin, T. J., Jan, Y. N., and Jan, L. Y. (1993) *Nature* **362,** 127–133
24. Morishige, K., Takahashi, N., Findlay, I., Koyama, H., Zanelli, J. S., Peterson, C., Jenkins, N. A., Copeland, N. G., Mori, N., and Kurachi, Y. (1993) *FEBS Lett.* **336,** 375–380
25. Gersch, M., Mutig, K., Bachmann, S., Kumar, S., Ouyang, X., and Johnson, R. (2006) *Nephrol. Dial. Transplant.* **21,** 2028–2029
26. Bachmann, S., Mutig, K., Bates, J., Welker, P., Geist, B., Gross, V., Luft, F. C., Alenina, N., Bader, M., Thiele, B. J., Prasadan, K., Raffi, H. S., and Kumar, S. (2005) *Am. J. Physiol. Renal Physiol.* **288,** F559–F567
27. Tamm, I., and Horsfall, F. L., Jr. (1950) *Proc. Soc. Exp. Biol. Med.* **74,** 106–108
28. Caldwell, S. R., Hill, K. J., and Cooper, A. A. (2001) *J. Biol. Chem.* **276,** 23296–23303
29. Haass, F. A., Jonikas, M., Walter, P., Weissman, J. S., Jan, Y. N., Jan, L. Y., and Schuldiner, M. (2007) *Proc. Natl. Acad. Sci. U.S.A.* **104,** 18079–18084
30. Powers, J., and Barlowe, C. (1998) *J. Cell Biol.* **142,** 1209–1222
31. Nakanishi, H., Suda, Y., and Neiman, A. M. (2007) *J. Cell Sci.* **120,** 908–916
32. Koh, K., Joiner, W. J., Wu, M. N., Yue, Z., Smith, C. J., and Sehgal, A. (2008) *Science* **321,** 372–376
33. Takiue, Y., Hosoyamada, M., Yokoo, T., Kimura, M., and Shibasaki, T. (2008) *Biol. Pharm. Bull* **31,** 405–411
34. Welker, P., Böhlick, A., Mutig, K., Salanova, M., Kahl, T., Schlüter, H., Blottner, D., Ponce-Coria, J., Gamba, G., and Bachmann, S. (2008) *Am. J. Physiol. Renal Physiol.* **295,** F789–802
35. Romanenko, V. G., Fang, Y., Byfield, F., Travis, A. J., Vandenberg, C. A., Rothblat, G. H., and Levitan, I. (2004) *Biophys. J.* **87,** 3850–3861
36. Cukras, C. A., Jeliazkova, I., and Nichols, C. G. (2002) *J. Gen. Physiol.* **119,** 581–591
37. Lu, M., Wang, T., Yan, Q., Wang, W., Giebisch, G., and Hebert, S. C. (2004) *Am. J. Physiol. Renal Physiol.* **286,** F490–F495
38. Wang, W. H. (2006) *Am. J. Physiol. Renal Physiol.* **290,** F14–F19
39. Chatterjee, S., and Mayor, S. (2001) *Cell Mol. Life Sci.* **58,** 1969–1987
40. Wolf, M. T., Mucha, B. E., Attanasio, M., Zalewski, I., Karle, S. M., Neumann, H. P., Rahman, N., Bader, B., Baldamus, C. A., Otto, E., Witzgall, R., Fuchshuber, A., and Hildebrandt, F. (2003) *Kidney Int.* **64,** 1580–1587
41. Okamoto, M., Yoko-o, T., Umemura, M., Nakayama, K., and Jigami, Y. (2006) *J. Biol. Chem.* **281,** 4013–4023